Video Article

Bio-layer Interferometry for Measuring Kinetics of Protein-protein Interactions and Allosteric Ligand Effects

Naman B. Shah[1], Thomas M. Duncan[1]

[1]Department of Biochemistry and Molecular Biology, SUNY Upstate Medical University

Correspondence to: Thomas M. Duncan at duncant@upstate.edu

URL: https://www.jove.com/video/51383
DOI: doi:10.3791/51383

Keywords: Chemistry, Issue 84, ATP synthase, Bio-Layer Interferometry, Ligand-induced conformational change, Biomolecular Interaction Analysis, Allosteric regulation, Enzyme inhibition

Date Published: 2/18/2014

Citation: Shah, N.B., Duncan, T.M. Bio-layer Interferometry for Measuring Kinetics of Protein-protein Interactions and Allosteric Ligand Effects. *J. Vis. Exp.* (84), e51383, doi:10.3791/51383 (2014).

Abstract

We describe the use of Bio-layer Interferometry to study inhibitory interactions of subunit ε with the catalytic complex of *Escherichia coli* ATP synthase. Bacterial F-type ATP synthase is the target of a new, FDA-approved antibiotic to combat drug-resistant tuberculosis. Understanding bacteria-specific auto-inhibition of ATP synthase by the C-terminal domain of subunit ε could provide a new means to target the enzyme for discovery of antibacterial drugs. The C-terminal domain of ε undergoes a dramatic conformational change when the enzyme transitions between the active and inactive states, and catalytic-site ligands can influence which of ε's conformations is predominant. The assay measures kinetics of ε's binding/dissociation with the catalytic complex, and indirectly measures the shift of enzyme-bound ε to and from the apparently nondissociable inhibitory conformation. The Bio-layer Interferometry signal is not overly sensitive to solution composition, so it can also be used to monitor allosteric effects of catalytic-site ligands on ε's conformational changes.

Video Link

The video component of this article can be found at https://www.jove.com/video/51383/

Introduction

Protein-protein interactions are important for many biological processes, and label-free optical methods like Surface Plasmon Resonance (SPR) have been used *in vitro* to study kinetics of binding and dissociation[1]. Most label-free methods immobilize one biomolecule on a sensor surface and use an optical signal to detect a binding partner from solution as it associates with the immobilized biomolecule[1]. While SPR is a highly sensitive method, it is prone to interference due to changes in the refractive index of the solution flowing over the sensor[2]. Although not as sensitive as SPR, Bio-layer Interferometry (BLI) is less affected by changes in sample composition[1,3]. BLI uses fiber optic biosensors that have a proprietary biocompatible coating at the tip. The system used here (Octet-RED96) contains eight spectrophotometers. White light is piped to a row of probes that move on a robotic arm. Fiber optic sensors are picked up by the probes and moved to a 96-well plate containing samples. One of the target molecules is immobilized on the biosensor surface. Then sensors are moved to wells containing the binding partner in solution. BLI monitors association of the binding partner with the immobilized molecule, and then monitors dissociation after moving the sensors to solution without the binding partner. Binding of molecules to the biosensor surface leads to changes in optical interference between light waves that reflect back to the spectrophotometers from an internal surface and from the external interface between sensor and solution. These changes in interference can be quantified and used to determine kinetic rates of binding and dissociation, as summarized in the animation of **Figure 1**.

We have applied BLI to measure interactions between the catalytic complex of bacterial ATP synthase and its ε subunit, which can auto-inhibit the enzyme. ATP synthase is a membrane-embedded rotary nanomotor that catalyzes synthesis and hydrolysis of ATP[4]. The catalytic complex (F_1) can be isolated in a soluble form that works as an ATPase. Subunit ε has two domains: the N-terminal domain (NTD) is necessary for proper assembly and functional coupling of the enzyme but does not interact directly with the catalytic subunits; the C-terminal domain (CTD) can inhibit the enzyme by interacting with multiple catalytic subunits[5,6]. This ε-mediated regulation is specific to bacterial ATP synthases and is not observed in the mitochondrial homologue. ATP synthase has emerged as a target for antibacterial drugs, as shown by recent FDA approval of bedaquiline to treat drug-resistant tuberculosis[7]. Thus, targeting ε's inhibitory role for drug discovery could yield antibacterials that do not inhibit the mitochondrial ATP synthase. With the isolated catalytic complex (F_1), ε becomes a dissociable subunit. However, with ε bound to F_1, the εCTD can undergo a dramatic conformational change, partially inserting into the enzyme's central cavity and forming an inhibitory state that is unlikely to dissociate directly[6,8]. We use BLI to measure kinetics of F_1/ε binding and dissociation, and indirectly, to examine allosteric effects of catalytic-site ligands on ε's conformation.

In our system, ε was chosen for immobilization on the sensor surface since BLI signal (like SPR) is sensitive to the mass of the molecules binding at the surface. The ε subunit is small (~15 kDa) relative to the main F_1 complex (~347 kDa). Thus, a larger BLI signal will result from binding of F_1 to immobilized ε. In order to monitor F_1 dissociation, which can be very slow, ε must be strongly immobilized. Thus we chose to biotinylate and immobilize it on streptavidin-coated biosensors. Proteins can be biotinylated by (i) random modification of surface lysines[9], (ii) reaction of a unique native or engineered cysteine with a biotin-maleimide reagent[10] or (iii) genetically adding a specific biotin-acceptor peptide

that is enzymatically biotinylated during *in vivo* expression of the tagged protein[11]. In our system, ε is biotinylated using method (iii)[8]. Once biotin-tagged ε is immobilized on streptavidin sensors, BLI can measure the binding and dissociation of F_1 that has been depleted of subunit ε (F_1(-ε)). For the experiments described here, preliminary assays had been done to determine reasonable amounts of the biotinylated protein to immobilize on the sensors. This can vary, depending on the molecular weight of the protein and its binding partner, but the goal is to determine a minimal amount of immobilized protein that provides (i) acceptable signal-to-noise for binding kinetics with a low concentration of the binding partner (below K_D) and (ii) minimal distortion of binding kinetics with near-saturating concentration of the binding partner. Also, stoichiometry of biotinylation may vary (but avoid >1 mol biotin/mol protein), so some initial assay may be needed for each new lot of biotinylated protein to confirm that a consistent BLI signal can be achieved during immobilization on the streptavidin-coated sensors.

Protocol

1. Programming the Instrument for BLI Assay

Turn on the instrument at least one hour in advance to allow the lamp to warm up; this is necessary to minimize noise and drift in optical signal during the experiment. Set the desired temperature via the instrument tab to prewarm the sample plate holder. Then set up the experimental design in the Data Acquisition software. Select "New Kinetics Experiment" in the Experiment Wizard tab. This presents a tabbed menu with all steps that must be defined.

1.1. Plate Definition

Define the columns to be used on the 96-well sample plate. Assign columns to contain buffer, immobilized protein or binding partner. For each association well, enter the concentration of binding partner to be used. Note: the plate definition shown in **Figure 2** has options for distinct assays.

1.2. Assay Definition

Define all steps needed for the assay. These include (i) Baseline (several), (ii) Loading, (iii) Association and (iv) Dissociation of binding partner. Then, as described below, link individual assay steps with columns of wells on the sample plate by selecting the assay step and then double clicking on the respective column. This programs the sensors to be moved from one column of wells to the next during the assay.

1. **Baseline**
   Begin with a brief baseline step (≥60 sec), with sensors in assay buffer (**Figure 2**, column 1), to establish initial BLI signals in the 96-well plate.
2. **Loading** (immobilizing the biotinylated protein on the sensors)
   Assign sensors to wells that will contain the biotinylated protein (**Figure 2**, column 2). Use the threshold function to achieve a predetermined level of binding (see Introduction). Set the threshold option so that all sensors will be moved to the next column of wells when any one of the sensors reaches the threshold.
3. **Baseline**
   Include another baseline step in buffer (**Figure 2**, column 3; typically >5 min) to wash away nonimmobilized biotinylated proteins from the sensors and establish new, stable baseline signals. For basic binding/dissociation assays only (as in **Figure 3**), include an extra baseline step (60 sec) with sensors in new wells of buffer (**Figure 2**, column 4) before the Association step.
4. **Association** (of the binding partner to the immobilized protein)
   For a basic binding/dissociation assay (as in **Figure 3**), select a range of concentrations of binding partner to be used for different sensors/wells (**Figure 2**, column 5). Adjust the step time so that at least a saturating concentration of the binding partner should approach equilibrium binding signal. For an assay to test allosteric effects of small ligands on dissociation of the protein-protein complex (as in **Figure 5**), select a single high concentration of binding partner (~10-fold above the estimated K_D) for use in all association wells.
5. **Dissociation** (of the binding partner)
   For a basic binding/dissociation assay only (as in **Figure 3**), designate the sensors to return to column 4 (**Figure 2**), the same buffer wells as used for the extra baseline before Association. For an assay to test allosteric effects of small ligands, instead designate sensors to move to column 6 (**Figure 2**), where each well can contain buffer plus different allosteric ligands.

1.3. Sensor Assignment

Indicate the locations in the sensor tray that will contain prewetted sensors for the assay. Identify any empty positions since the experiment will fail if no sensors are picked up.

1.4. Review Experiment

Visualize all planned steps to check for mistakes and go back to correct them.

1.5. Run Experiment

Enter necessary details, including location of data files. Enter the desired temperature for the experiment. If sensors still require prewetting, select the option to delay starting the experiment. Finally, once all sample preparation is complete (step 2) and both the sample plate and sensor tray are loaded in the instrument , click the Go button to run the assay.

2. Sample Preparation

1. Prepare an appropriate assay buffer. Buffer used for experiments shown in **Figures 3** and **5**: 20 mM MOPS (3-(N-Morpholino)propanesulfonic acid), Tris (Tris(hydroxymethyl)amino-methane) (added to adjust pH to 8.0), 50 mM KCl. Include BSA (bovine serum albumin, fatty-acid free, 0.5 mg/ml final) in the buffer for all assay steps and for all dilutions of the biotinylated protein or binding partner to minimize nonspecific binding of proteins to the sensors.
2. Dilute the biotinylated protein (ε) in assay buffer to an appropriate concentration (see Introduction).
3. Prepare dilutions of the binding partner (F_1(-ε)) in assay buffer (see Discussion for range of concentrations to use).
4. Prewet the streptavidin-coated sensors for at least 10 min to remove their protective sucrose coating. Remove the sensor-containing rack from the sensor tray and insert a 96-well plate in the bottom of the tray, sliding one corner of the plate into the orienting notch on the tray. For the column of sensors to be used, add 200 µl of assay buffer per well in that column of the 96-well plate. Return the rack of sensors to the tray in the correct orientation (with tabs in slots).
5. As assigned during programming in Step 1, fill wells of the sample plate with assay buffer or the appropriate protein dilutions, as in **Figure 2**. Avoid introducing bubbles, as they can cause noise in the optical signal. Include one or more reference wells that omit either (i) biotinylated protein or (ii) binding partner.
6. Open the door of the instrument and insert the sensor tray onto the stage (left), with the tray's tabs inserted into the slots of the stage. Insert the sample plate into the plate holder (right); make sure that the plate is seated flat and in the correct orientation, as indicated on the plate holder. Close the door and start the assay from the Data Acquisition program (step 1.5).

3. Data Processing

1. After the assay has run, open the Data Analysis software and load the folder containing the data. Click the "Processing" tab to see a step-wise Processing menu (at left) and the raw kinetic data, with each sensor (A-H) assigned a different color (see **Figure 3**).
2. Under "Data Selection", click the "Sensor Selection" button. On the "Sample Plate Map", designate the wells for 1 or 2 control sensors (G, H in assay of **Figure 3**) as reference wells. On the Processing menu, check the "Subtraction" box and select "Reference Wells" to subtract reference signal (single or averaged) from every other sensor's signal.
3. Align all traces to Y=0 by using the "Align Y Axis" step. Select "Baseline" as the alignment step (this being the last baseline before the Association step). For "Time Range", enter the last 10 sec of that baseline (*i.e.* 50-60 sec for a 60-sec baseline, as in **Figure 3**).
4. Check the "Inter-step Correction" box to minimize signal shifts between the Association and Dissociation steps. Select align to Baseline or Dissociation.
5. Select Savitzky-Golay filtering function in most cases and click "Process Data!" to proceed. Visually inspect the final processed data (lower right panel). With assays intended for global data analysis (as in **Figure 4**), if signal traces show a significant shift between Association and Dissociation steps, change the selection of Dissociation or Baseline for the "Inter-step Correction" and reprocess the data before proceeding to Data Analysis.

4. Data Analysis

Click the "Analysis" tab in Data Analysis to begin. Note: the example steps below are for global analysis of multiple binding/dissociation curves (as in **Figure 3**).

1. For "Step to Analyze", choose Association and Dissociation. For "Model", select 1:1. Note: other limited options are available.
2. For "Fitting", choose Global (Full). For "Group By" select Color (as on the graph). Select "R_{max} Unlinked By Sensor" to allow independent fitting of R_{max} (maximal signal response upon saturating binding of the partner to the immobilized protein). Note: we do this for most assays, as sensors vary slightly in the amount of protein immobilized (see **Figure 3**, Loading).
3. On the table shown, make sure all sensor traces to be analyzed have the same color, so they will be analyzed as a global set. If needed, select one or more sensor traces to omit from global fitting: under the "Include" column, right-click on the desired sensor position and select "Exclude Wells".
4. Click "Fit Curves!" to start the nonlinear regression analysis. Examine the fitting results, which include (i) overlay of regression curves with sensor data traces (as in **Figure 4**), (ii) plots of fitting residuals, and (iii) a table with determined parameter values (rate constants, R_{max}, K_D) and statistics (standard errors for parameters, Chi-squared, R^2).
5. Under "Data Export", save fitting results by clicking "Export Table to .csv File". For graphing or further analysis of data/fitted curves with other software, click "Export Fitting Results" to save each sensor's data and fitted curve in a text file.

Representative Results

Real time binding and dissociation BLI kinetics are shown in **Figure 3**. This experiment was done with assay buffer in association and dissociation. This experiment was started with a 10 min baseline step since the sensors had been prewet only briefly. Next, biotinylated ε was loaded on the sensors. No detectable dissociation of ε occurred throughout all remaining steps as seen from the reference curve (G) which had no binding partner added. A second reference sensor (H) was devoid of immobilized protein and showed low nonspecific binding of the binding partner. Various concentrations of F_1(-ε) were used in the association step for sensors A-F in order to fit results globally and get the best values for k_a, k_d, and K_D. Results were processed as in the protocol, yielding the data traces (blue) in **Figure 4**. In this case, reference sensor trace H was subtracted from sample traces to correct for nonspecific binding of the binding partner and system signal drift. In the data analysis step, all curves were globally fit with a 1:1 model (single k_a, single k_d); the "Global (Full)" fit assumes complete dissociation of the binding partner (signal will return to zero at infinite time) (**Figure 4**, red). Note that, for the two highest concentrations of F_1(-ε), there are small but significant deviations of the data from the global, 1:1 model. Low levels of immobilized ligand (biotinylated "ε" subunit) were used, and the fit was not improved by including a mass transport factor in the model (not shown). However, F_1(-"ε") is a large complex (~350 kDa), and other experiments

(not shown) suggest that these deviations are due to reduced binding accessibility of a fraction of immobilized ligand; *i.e.* an F_1 bound to one "ε" may sterically hinder access to another biotinylated "ε" bound on the same streptavidin tetramer.

Figure 5 shows a different experiment in which the enzyme was bound to sensor-immobilized ε in the presence of 1 mM ATP/EDTA; this predisposes most F_1/"ε" complexes to assume the noninhibitory conformation, which dissociates readily[8]. Sensors were then moved to dissociation wells containing assay buffer with different ligands. This demonstrates the effects of different ligands on the conformation of ε. For example, exposure to MgADP/Pi dramatically slowed net dissociation, indicating that ε shifted conformation to the tightly-bound, inhibitory state. Complex dissociation kinetics were observed since different ligands caused different shifts in the fraction of F_1.ε complexes with ε in the active (dissociable) or inhibitory (nondissociable) conformations. It is also possible that substantial conformational changes of bound proteins contribute directly to changes in BLI signal but, in our studies, this appears to be negligible compared to the signal for binding/dissociation of the large F_1 complex (see Shah *et al.*[8], Figure 5D; transition to curves 3 and 6 show very similar behavior, although their conditions favor distinct conformations of bound F_1). The Data Analysis software was not designed for such complex dissociation kinetics. Thus, we exported the data to text files for nonlinear regression analysis with other software.

Figure 1. Principles of Bio-layer Interferometry. Animation summarizes the underlying physics for detecting biomolecular interaction by BLI. Light passing through the probes is reflected back to the spectrophotometers (i) from the internal surface of the sensor and (ii) from the external interface of the sensor with the sample solution. This results in an interference pattern. Binding of molecules to the sensor surface changes the interference pattern. This can be plotted as a nanometer shift of relative intensity *vs* wavelength. Monitoring this nanometer shift over time provides binding and dissociation kinetics. Graphics are adapted with permission from FortéBio[12].

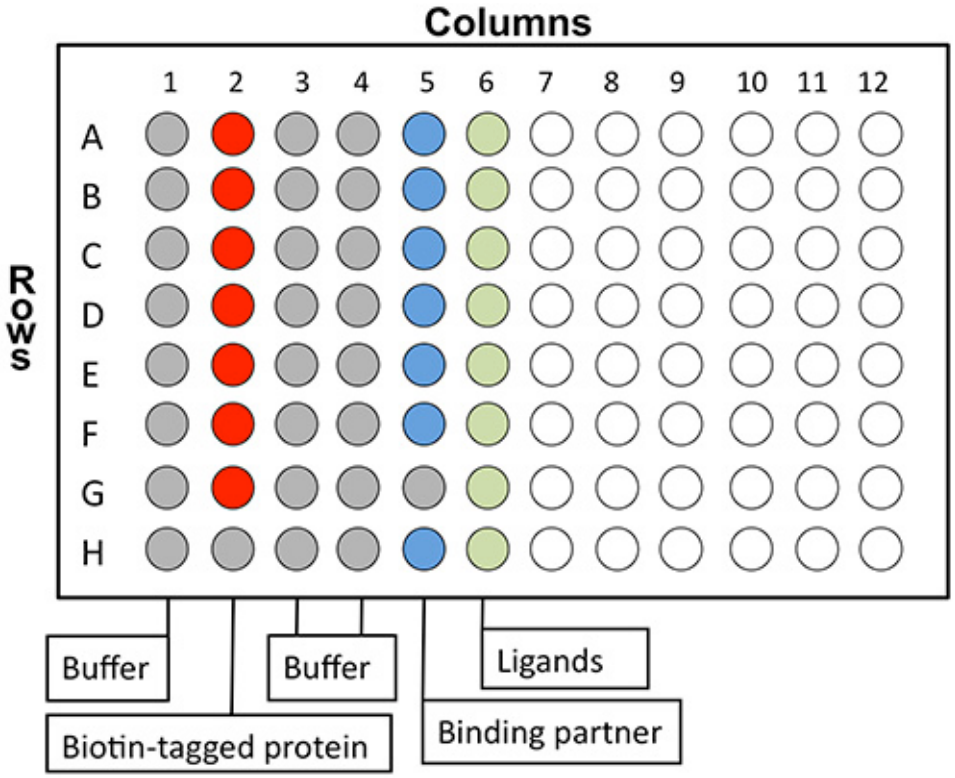

Figure 2. Schematic arrangement of samples in the 96-well sample plate. The sensors will be moved in parallel from column to column and can be moved either left or right as defined in a particular assay protocol. Wells with grey color represent assay buffer whereas red, blue and green represent immobilized protein, binding partner and ligands, respectively.

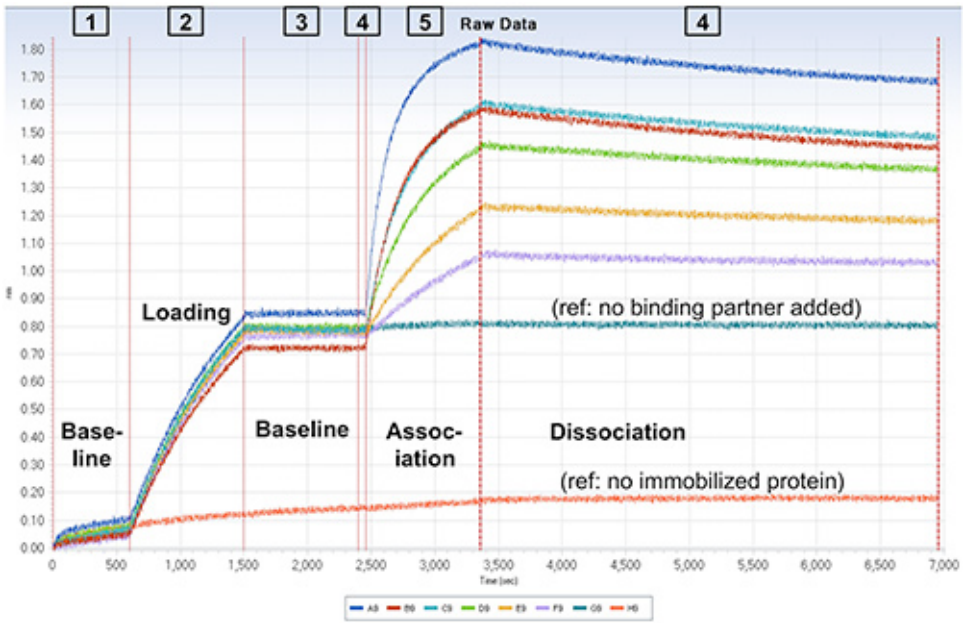

Figure 3. Screen capture showing raw data from a BLI assay. Vertical red lines indicate movement of sensors between assay steps of the protocol. Step types are denoted on the image. Locations of buffer and samples are as shown in **Figure 2**. As noted by numbers along the top of the graph, streptavidin-coated sensors were moved between different columns of the sample plate in the following order: 123454. The legend below the graph indicates the color for each sensor's data trace. In the Loading step, each sensor except H was incubated with 50 nM biotinylated "ε" subunit. In the Association step, sensors were incubated with nM concentrations of "ε"-depleted F_1: 30 (A, H), 20 (B), 15 (C), 10 (D), 5 (E), 2.5 (F), 0 nM (G). Click here to view larger image.

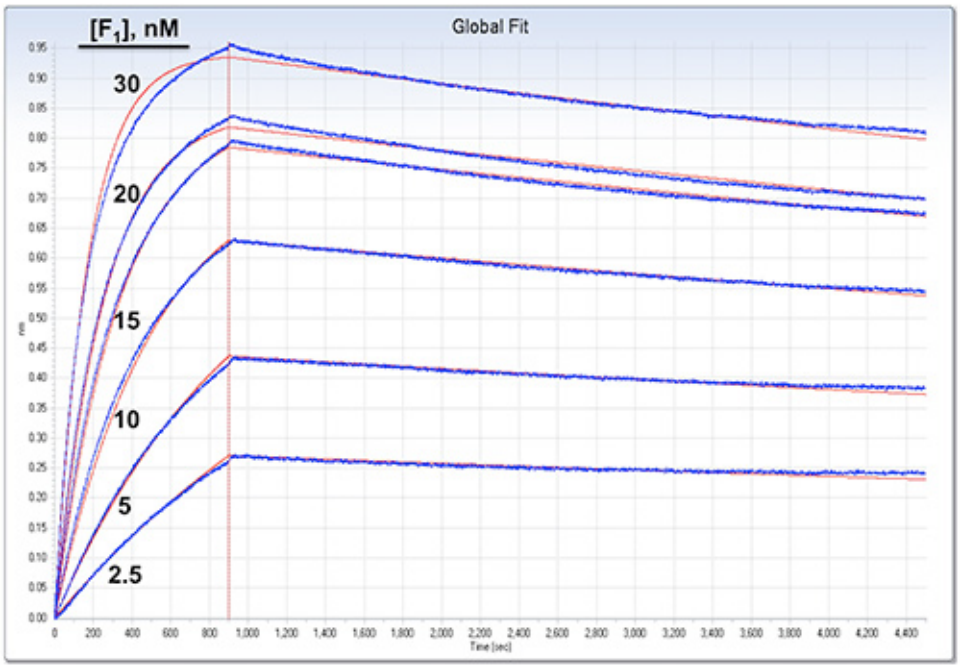

Figure 4. Screen capture of the analyzed data from the BLI assay of Figure 3. The data was processed and fitted as described in the text. Only Association and Dissociation steps are shown, divided by a vertical red line. The processed data curves are blue; the nonlinear regression fits from 1:1 global analysis are shown in red. Global fitting results[8]: k_a = 2 x 10^5 $m^{-1}s^{-1}$ (±0.1%), k_d = 4.8 x 10^{-5} s^{-1} ("±"0.1%), yielding K_D = 0.24 nM. Goodness of fit: R^2 = 0.999054. The maximal binding parameter (R_{max}) was fit separately for each sensor, with mean value = 0.813 nm ("±"0.0803). Click here to view larger image.

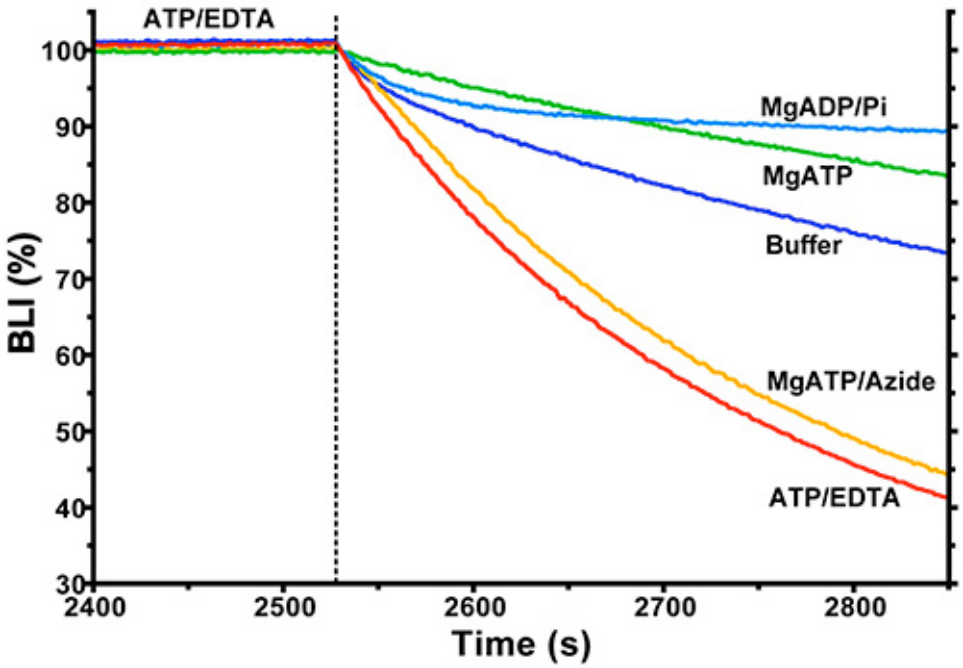

Figure 5. Results from a BLI assay showing allosteric effects of ligands on ε's conformation. F_1(-ε) was bound to sensor-immobilized ε in the presence of 1 mM ATP/EDTA. The end of the association phase and a portion of the dissociation phase are shown. During the dissociation step, distinct ligands for F_1 catalytic sites (listed for each trace) were included to observe their allosteric effects on dissociation of F_1 from sensor-bound ε.

Discussion

Currently available instruments for BLI allow significant throughput and flexibility in assays for biomolecular interactions. Various solution samples are dispensed in wells of a black microtiter plate, and a set of parallel BLI sensors are programmed to move back and forth between columns of wells on the plate. The samples are stirred by orbital shaking throughout the assay. The system used here has 8 sensors and uses a 96-well sample plate, but another system uses 16 sensors and a 384-well sample plate. Thus, interaction between a sensor-immobilized biomolecule and its binding partner in solution can be tested under different conditions with multiple sensors in parallel. For example, in the first assay presented here with the immobilized inhibitory ε subunit, interactions were measured with six different concentrations of the enzyme (binding partner) in parallel (**Figures 3** and **4**). This allowed a global analysis to determine a single pair of rate constants (k_a, k_d) for net binding and dissociation, and thus an equilibrium dissociation constant ($K_D = k_d/k_a$), which agrees closely with the inhibitory constant (K_I) determined from solution assays of enzyme inhibition by ε[8]. A second type of experiment (**Figure 5**) demonstrated that BLI can also monitor allosteric effects of small ligands on the interactions between two proteins; the effects of different ligands were compared in parallel. There are limitations for detecting effects of allosteric ligands, since BLI signal depends on the mass of the binding molecule, and can directly detect binding of small compounds under optimized conditions[13]. However, in the assay of **Figure 5**, the binding partner, F_1, was a large protein complex (~347 kDa), so the BLI signal for its binding/dissociation was not significantly affected by additional binding of small ligands such as ATP (~500 Da) to the F_1 complex. This was confirmed with assays in which these ligands did not affect the BLI signal for F_1 bound to a truncated form of ε lacking the inhibitory CTD[8]. Thus, assays of allosteric effects must consider the mass of the allosteric ligand relative to the masses of the interacting proteins, and preferably include controls to test for direct BLI response to the binding of the ligand.

Note that certain steps and modifications in the experimental protocol can be critical for achieving better results and more accurate analysis. For example, as in the protocol described here (see steps 1.2.3, 1.2.5), an assay intended for global analysis of binding and dissociation rate constants should include an extra baseline step (see step 1.2.3) in a new column of buffer wells (**Figure 2**, column 4) before the Association step, and the sensors should be returned to that same column of buffer wells for the Dissociation step (see step 1.2.5). Having each sensor in the same well (with the same optical properties) before and after the Association step can improve the inter-step correction (step 3.4) for Association/Dissociation steps, and this facilitates global kinetic fitting of multiple data traces (as in **Figure 4**). Also, for assays that are more preliminary than shown here, the program has an option to shorten or extend the time of any step during the assay (while it is the active step). This is useful, for example, if the optimal loading signal is not already known, or if more time is needed to allow enough dissociation to achieve a good fit for the dissociation rate.

Nonspecific binding of the binding partner to the sensor surface can be a problem for label-free methods such as SPR and BLI. In our assays, this was effectively minimized by including BSA in the assay buffer. As in immunoblotting protocols, proteins other than BSA could be used, and low concentrations of detergent may also minimize nonspecific binding (Tween20 is used in kinetics buffer from the supplier). Even with minimal nonspecific binding, most assays should include at least one control sensor without immobilized protein but with the highest concentration of binding partner in the Association step (see **Figure 3**, sensor H); subtraction of the residual nonspecific binding (and its decay during the Dissociation step) can significantly improve kinetic analyses for the specific binding/dissociation being studied. On the other hand, once initial assays confirm that the biotinylated protein remains stably bound after the Loading step (see **Figure 3**, sensor G), that control can be omitted and that sensor can be used for a sample condition.

For robust determination of association and dissociation rate constants using BLI, multiple concentrations of binding partner should be used and all the data traces should be fit by global analysis, if possible (as in **Figures 3** and **4**). Ideally, the range of concentrations should span ~10-fold above and below the estimated K_D. In our case, with a high-affinity interaction (K_D =0.25 nM), the signal-to-noise was poor for binding kinetics with sub-K_D concentrations. Thus, concentrations of binding partner above the K_D were used such that significant changes in observed rates and levels of binding were obtained (see **Figure 3**). Also, a long dissociation step was used to improve the confidence in fitting the slow dissociation rate. With high affinity interactions, it is also possible that slow dissociation is exaggerated by rebinding during the dissociation step, since BLI assays are done in a stirred sample rather than continued flow over the sensor, as for SPR. This potential artifact can be tested with assays in which the dissociation buffer contains a 'sink' of excess competitive protein that binds dissociated binding partner and prevents it from rebinding to the sensor-immobilized protein[14]. In our system, this was done by comparing results with and without nonbiotinylated (>10-fold above K_D) in the dissociation well, and we confirmed that rebinding was not a significant problem[8]. Finally, if sets of kinetic results are not fit well by global analysis (1:1 or 2:1 models available), there are other analysis options for troubleshooting. For example, instead of choosing "Global (Full)" (in step 4.2), "Local" can be chosen to fit each sensor trace independently. If binding follows a simple 1:1 model, plotting the observed binding rates (k_{obs}) *vs* the concentrations of binding partner should show a linear dependence, with the slope equal to the second-order, intrinsic binding rate. The Analysis tab of the software has an "X-Y graph" window that allows quick visualization of this relationship.

One limitation of the instrument that we used is the available temperature range. With a range of 2 °C above ambient temperature to 40 ºC, only molecules that are stable in that range can be used. Moreover, thermodynamic analysis is limited by the narrow temperature range. Another general limitation is that the maximum assay time is ~4 hr; after this, artifacts develop due to evaporation of samples from the open microtiter plate.

BLI involves a relatively simple arrangement compared to SPR. The sensors are moved between columns of wells with fixed volumes, rather than a constant flow of sample over the sensor. Although not as sensitive as SPR, BLI is less affected by changes in refractive index due to changes in sample composition. Overall, with this relative ease of use and flexibility of the instrument in shifting between assay conditions, BLI provides a versatile tool for *in vitro* assays of biomolecular interactions.

Disclosures

The authors declare that they have no conflicts of interest.

Acknowledgements

We thank FortéBio for providing graphics used in **Figure 1**. This work was supported by NIH grant GM083088 to T.M.D.

References

1. Nirschl, M., Reuter, F., Voros, Janos. Review of Transducer Principles for Label-Free Biomolecular Interaction Analysis. *Biosensors.* **1**, 70-92 (2011).
2. Homola, J. Present and future of surface plasmon resonance biosensors. . *Anal. Bioanal. Chem.* **377**, 528-539 (2003).
3. Piehler, J., Brecht, A. & Gauglitz, G. Affinity Detection of Low Molecular Weight Analytes. *Anal. Chem.* **68**, 139-143, doi:10.1021/ac9504878 (1996).
4. Duncan, T. M. in *The Enzymes, vol. XXIII: Energy Coupling and Molecular Motors* Vol. 23 eds D.D. Hackney & F. Tamanoi. Elsevier Academic Press, 203-275 (2004).
5. Feniouk, B. A., Suzuki, T. & Yoshida, M. The role of subunit ε in the catalysis and regulation of FOF1-ATP synthase. *Biochim. Biophys. Acta.* **1757**, 326-338 (2006).
6. Cingolani, G. & Duncan, T. M. Structure of the ATP synthase catalytic complex (F1) from *Escherichia coli* in an autoinhibited conformation. *Nat. Struc. Mol. Biol.* **18**, 701-707, doi:doi:10.1038/nsmb.2058 (2011).
7. Mirsaeidi, M. After 40 years, new medicine for combating TB. *Int. J. Mycobacteriol.* **2**, 1-2 (2013).
8. Shah, N. B., Hutcheon, M. L., Haarer, B. K. & Duncan, T. M. F1-ATPase of Escherichia coli: The ε-inhibited state forms after ATP hydrolysis, is distinct from the ADP-inhibited state, and responds dynamically to catalytic site ligands. *J. Biol. Chem.* **288**, 9383-9395 (2013).
9. Burgess, T. L., Ross, S. L., Qian, Y.-x., Brankow, D. & Hu, S. Biosynthetic Processing of neu Differentiation Factor: glycosylation, trafficking, and regulated cleavage from the cell surface. *J. Biol. Chem.* **270**, 19188-19196 (1995).
10. Loo, T. W. & Clarke, D. M. Membrane Topology of a Cysteine-less Mutant of Human P-glycoprotein. *J. Biol. Chem.* **270**, 843-848 (1995).
11. Tsao, K.-L., DeBarbieri, B., Michel, H., and Waugh, D. S. A versatile plasmid expression vector for the production of biotinylated proteins by site-specific, enzymatic modification in *Escherichia coli. Gene.* **169**, 59-64 (1996).
12. Dayne, D. BioLayer Interferometry (BLI) – How Does it Work? FortéBio newsletter: *In Interactions.* **5**, 8-9 (2012).
13. Wartchow, C. *et al.* Biosensor-based small molecule fragment screening with biolayer interferometry. *J. Comput. Aided Mol. Des.* **25**, 669-676, doi:10.1007/s10822-011-9439-8 (2011).
14. Abdiche, Y., Malashock, D., Pinkerton, A. & Pons, J. Determining kinetics and affinities of protein interactions using a parallel real-time label-free biosensor, the Octet. *Anal. Biochem.* **377**, 209-217, doi:http://dx.doi.org/10.1016/j.ab.2008.03.035 (2008).

